Colloid Polym Sci (2009) 287:45–55
DOI 10.1007/s00396-008-1951-6

ORIGINAL CONTRIBUTION

Synthesis of amphiphilic diblock copolymers poly[2-(*N*, *N*-dimethylamino)ethyl methacrylate]-*b*-poly (stearyl methacrylate) and their self-assembly in mixed solvent

Cuicui Liu · Peihong Ni · Xiao Fang · Xiaodong Zhou

Received: 26 June 2008 / Revised: 8 October 2008 / Accepted: 15 October 2008 / Published online: 4 November 2008

Abstract Amphiphilic diblock copolymers consisting of 2-(*N*, *N*-dimethylamino)ethyl methacrylate (DMAEMA, abbreviated as DMA) and stearyl methacrylate (SMA) with different degrees of polymerization and compositions were prepared by reversible addition–fragmentation chain transfer (RAFT) copolymerization. The composition and chemical structures of (co)polymers were confirmed by the measurements of ^{1}H NMR spectroscopy and gel permeation chromatography (GPC). The self-aggregating structures of amphiphilic diblock copolymers with the concentration of 0.1~0.3 wt.% in THF/water mixed solvent was investigated by transmission electron microscopy (TEM) and dynamic light scattering (DLS). It was found that both the morphologies and aggregating particle size resulted from the amphiphilic diblock copolymers depended on the variation of pH values, the lengths of the hydrophobic PSMA chains, and the weight ratio of THF/water mixed solvent.

Keywords Amphiphilic copolymer · 2-(*N* · *N*-dimethylamino)ethyl methacrylate · Stearyl methacrylate · RAFT polymerization · Self-assembly

C. Liu · P. Ni (✉) · X. Fang · X. Zhou
Key Laboratory of Organic Chemistry of Jiangsu Province, College of Chemistry, Chemical Engineering and Materials Science, Soochow University,
Suzhou 215123, China
e-mail: phni@suda.edu.cn

Introduction

In recent years, considerable attentions have been focused in preparing the amphiphilic block copolymers because of their intriguing self-assembly behaviors in aqueous or mixed solvents. Also, various amphiphilic copolymers can result in abundant micelle morphologies (e.g., spheres, rods, lamella, vesicles, and large compound micelles), which have potential applications in nanoscience and nanotechnology, such as carriers for drug and gene delivery, diagnostic imaging, and nanoreactors [1–4].

As a sort of water-soluble and pH-sensitive polymer, poly[2-(*N*, *N*-dimethylamino)ethyl methacrylate] (PDMA) and its derivatives have many applications in various fields, including filtration techniques [5], coatings and surface patterning [6], and polymeric carrier [7, 8]. Controlled/living polymerization has been used to prepare PDMA-containing copolymers, especially the reversible addition fragmentation transfer (RAFT) polymerization technique [9–17]. For example, detailed researches on the well-controlled homopolymerization characters of 2-(*N*, *N*-dimethylamino)ethyl methacrylate (DMA) were conducted successfully both in dioxane [12] and water [13], and the resulting PDMA was further used in miniemulsion polymerization [13]. In addition, DMA monomer has been copolymerized with various hydrophilic or hydrophobic monomers, such as sodium acrylate (SA) [9], benzyl methacrylate (BzMA) [10], methyl methacrylate (MMA) [11], styrene (St) [14], poly(ethylene glycol) methyl ether methacrylate (PEGMA) [15], 3-*O*-methacryloyl-D-galactopyranose

(MAGP) [16], and *N*-isopropylacrylamide (NIPAM) [17], to design materials able to respond in a physiological environment [15, 16], and provide materials with potential diagnostic and targeting applications [17]. Our group has been working on the homopolymerization [13, 18, 19] and copolymerization [20–22] of DMA monomer for a long time. Recently, we have designed several amphiphilic PDMA-based copolymers. These copolymers exhibited interesting solution behaviors and various self-assembled morphologies in aqueous or selective solvents.

Stearyl methacrylate (SMA) is a unique monomer due to its pendent long alkyl side chain, which can form crystalline domain and can be used to synthesize comb-like polymers [23, 24]. Many studies have been performed on the synthesis and self-assembly of comb-like copolymers based on PSMA owing to their interesting solution behaviors [23, 25–28]. Wang et al. [26, 27] have synthesized poly(stearyl methacrylate)-*b*-poly(3-(trimethoxysilyl) propyl methacrylate) (PSMA-*b*-PTMSPMA) and poly (maleic anhydride-*alt*-stearyl methacrylat)-*b*-poly(stearyl methacrylate) [P(MA-*alt*-SMA)-*b*-PSMA] amphiphilic copolymers and obtained vesicles, core-shell spheres, and pearl-necklace-like aggregates from the copolymers in THF/water. Considering the special characteristic of SMA monomer, we attempted to combine the hydrophobic PSMA block with PDMA block to form a novel amphiphilic copolymer PDMA-*b*-PSMA. This copolymer should possess both properties of PSMA and PDMA (i.e., the comb-like, hydrophobic, and crystalline properties of PSMA, the pH-sensitive, and hydrophilic properties of PDMA). In acidic media, PDMA block can be protonated to yield polycationic segment and electrostatically stabilize micelles with the PSMA segments as the core. Moreover, it is well-known that pH-sensitive micelles could be used to confer bioadhesive properties and might have potential application in drug delivery by conjugating to drugs and responding to external stimuli [28–30]. With these in mind, the synthesis and aggregating behaviors of the novel comb-like copolymer PDMA-*b*-PSMA should be worthy to investigate in detail. Besides, to our knowledge, there was no report on the synthesis and self-assembly of amphiphilic copolymers containing both hydrophilic PDMA block and hydrophobic PSMA block.

In this paper, we have synthesized PDMA-*b*-PSMA diblock copolymers with different block lengths and then characterized these copolymers by ^{1}H NMR and GPC measurements. The aggregation morphologies depended on adjusting some parameters, such as polymer composition, solvent composition, and pH values, and were investigated by transmission electron microscopy (TEM) and dynamic light scattering (DLS). Scheme 1 outlines the representative synthesis route and the typical structure of PDMA-*b*-PSMA diblock copolymer.

Experimental

Materials

2-(*N*, *N*-dimethylamino)ethyl methacrylate (DMA) (Shanghai Chemical Reagent) was passed through a basic alumina column to remove the inhibitor and distilled from CaH_2 in vacuum before use. Stearyl methacrylate (SMA) (Aldrich) was purified by recrystallization in hexane. Other reagents, such as tetrahydrofuran (THF), *n*-hexane, hydroquinone, isopropyl alcohol, and ethanol, were reagent-grade and used

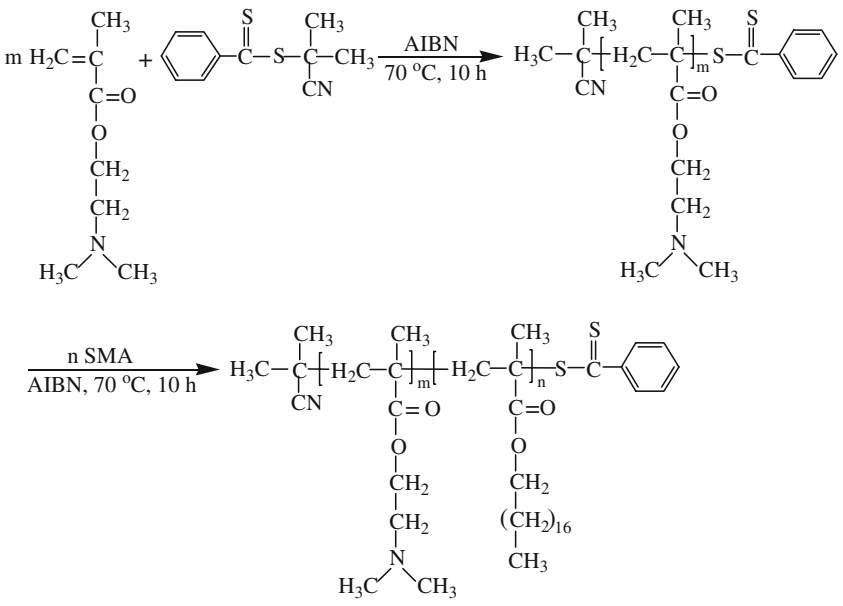

Scheme 1 A representative synthesis route for the PDMA homopolymers and PDMA-*b*-PSMA diblock copolymers via RAFT polymerization using isopropyl alcohol as solvent

as received. 2, 2′-Azobisisobutyronitrile (AIBN, Shanghai Chemical Reagent; 98%) was recrystallized from ethanol and kept in a refrigerator under 4 °C. 2-Cyanoprop-2-yl dithiobenzoate (CPDB) was synthesized according to the previous publication [31]. ^{1}H NMR (400 MHz, $CDCl_3$): δ 7.2–7.6 ppm (5H, aromatic H), 2.0 ppm [6H, –C(CN)($C\mathbf{H}_3$)$_2$].

RAFT polymerization of DMA

A homogeneous mixture of the monomer (DMA), initiator (AIBN), CTA (CPDB), and solvent (anhydrous isopropyl alcohol) was added to a three-necked round-bottomed flask fitted with a reflux condenser, a thermometer, and a nitrogen inlet. After the mixture was deoxygenated by purging with N_2 for half an hour, the flask was immersed into a thermostat at 70 °C, and the RAFT polymerization was carried out under a nitrogen atmosphere. Samples were periodically withdrawn from the reactor, immediately quenched with hydroquinone in an ice-water bath, and then dried in oven at 50 °C. The resultant products were used for gravimetric analyses and GPC measurements. The reaction was carried out for 10 h, and then the solvent was removed with a rotary vacuum distillatory. The crude product was purified by repeated precipitation into cold *n*-hexane and dried in a vacuum oven overnight. The purified PDMA homopolymers were obtained and could be used as the macro-CTA in the subsequent RAFT polymerization of the SMA monomer. The monomer/CTA/initiator molar ratios for the PDMA homopolymerization, the molecular weights, and the polydispersity indices (PDIs) of PDMA homopolymers are listed in Table 1.

RAFT polymerization of SMA with the PDMA macro-CTA

The second monomer SMA was mixed with the PDMA macro-CTA, initiator (AIBN), and anhydrous isopropyl alcohol under agitation until the mixture was homogeneous. The mixture was then added to a round-bottomed flask. After nitrogen was bubbled for half an hour, the flask was immersed into a preheated oil bath at 70 °C, and the polymerization was conducted for 10 h. The procedure for the purification of the PDMA-*b*-PSMA copolymers was almost the same with that for PDMA homopolymers. The [M]/[CTA]/[I] molar ratios and the polymerization results for PDMA-*b*-PSMA copolymers are listed in Table 1.

Self-assembly of the diblock PDMA-*b*-PSMA copolymers

The PDMA-*b*-PSMA diblock copolymer was first dissolved in THF with a desired concentration. Then, deionized water or aqueous solution of diluted hydrochloric acid with different pH values was dripped slowly to the copolymer solutions by syringe under vigorous agitation at room temperature. The copolymer concentration was kept at 0.1~0.3 wt.% in the resultant solution, and the water content ranged from 10 to 50 wt.% in the H_2O/THF mixed solvent. The micelle solution was stirred in sealed vials at

Table 1 Recipes, conversion, molecular weights and molecular weight distributions for the PDMA homopolymers and the PDMA-*b*-PSMA diblock copolymers synthesized via the RAFT polymerization in isopropyl alcohol at 70 °C

Run	Polymer[a]	[*M*]/[CTA]/[I] (molar ratio)[b]	Time (h)	Conversion (%)[c]	M_n (g mol^{-1})[d]	$M_{n,\,th}$ (g mol^{-1})[e]	PDI (M_w/M_n)[d]
1[f]	PDMA	100:3:1	12	23.5	–	–	–
2[f]	PDMA	100:3:1	11.5	23.5	–	–	–
3	$PDMA_{14}$	50:3:1	10	74.6	2,480	2,590	1.18
4	$PDMA_{14}$	50:3:1	10	83.9	2,430	2,880	1.21
5	$PDMA_{17}$	100:3:1	10	81.9	2,950	4,110	1.20
6	$PDMA_{17}$-*b*-$PSMA_{12}$	40:6:1	10	77.9	6,940	4,710	1.21
7	$PDMA_{17}$-*b*-$PSMA_{17}$	36:4:1	10	68.8	8,640	5,040	1.26
8	$PDMA_{18}$	100:3:1	10	74.1	3,110	3,720	1.20
9	$PDMA_{18}$-*b*-$PSMA_{13}$	36:4:1	10	60.6	7,620	4,950	1.26
10	$PDMA_{18}$-*b*-$PSMA_{27}$	37:5:1	10	80.0	12,060	5,110	1.34
11	$PDMA_{27}$	150:3:1	10	79.5	4,450	5,870	1.24
12	$PDMA_{27}$-*b*-$PSMA_{19}$	38:3:1	10	70.6	10,690	7,120	1.35

[a] The degrees of polymerization (average) were calculated from M_n

[b] [*M*] represents monomer concentration of DMA for homopolymerization and SMA for block copolymerization; [CTA] represents the concentration of CPDB or PDMA macro-CTA, if used; [*I*] means the concentration of AIBN

[c] For the homopolymerization, the monomer conversion was obtained by gravimetric method, while for the block copolymerization, it was calculated from ^{1}H NMR spectra

[d] Determined by GPC with THF as the eluent and standard polystyrene as calibration

[e] Calculated according to the equation mentioned in the part of the "Results and discussion" section

[f] The solvent used in Run 1 and 2 was ethanol, while isopropyl alcohol was employed in the others

room temperature for at least 1 day before measurement. Samples for TEM measurements were prepared by placing a drop of micelle solution onto 400-mesh carbon-coated copper grids, followed by air-drying at room temperature. For dynamic light scattering (DLS) measurement, these solutions were passed through 0.45 μm hydrophilic microfilters (Agilent Technologies) in a quartz sample cell.

Characterizations

The monomer conversion was determined by gravimetric method. During the reaction progress, samples were drawn from the reactor at interval times, immediately quenched with hydroquinone in an ice-water bath, and then dried in oven at 50 °C.

The molecular weight (M_n) and molecular weight distribution (PDI) of the dried polymers samples were measured on a Waters 1515 gel permeation chromatography (GPC) instrument equipped with a PLgel 5.0-μm-bead-size guard column (50×7.5 mm^2), followed by two linear PLgel columns (500 Å and Mixed-C) and a differential refractive-index detector. THF was employed as the eluent at a flow rate of 1.0 mL min^{-1}. Molecular weights of samples were determined with standard polystyrene calibration.

The chemical structures of the homopolymers and diblock copolymers were studied by ^1H NMR on an INVOA-400 nuclear magnetic resonance (NMR) instrument using $CDCl_3$ as solvent and tetramethylsilane (TMS) as the internal standard. Samples were dissolved in $CDCl_3$ at 10 mg mL^{-1} and measured at room temperature.

Transmission electron microscopy (TEM) was performed with instrument (TECNAI $G^2$20, FEI) at 200 KV. The micelle solution was placed onto 400-mesh carbon-coated copper grids, followed by air-drying at room temperature for 1 day before measurement.

The dynamic light scattering (DLS) measurements were performed with an HPPS (high performance particle sizer) 5001 high performance particle size instrument (Malvern) at 25 °C. All polymer solutions were prepared by the same method as for the TEM analysis and then passed through 0.45 μm microfilters before measurement. The cumulant method was chosen for measuring the *z*-average of the reciprocal diameter (D_z) and size polydispersity.

Results and discussion

CPDB-mediated RAFT homopolymerizations of DMA

2-Cyanoprop-2-yl dithiobenzoate (CPDB) was chosen as chain transfer agent (CTA) due to its high efficiency in the RAFT polymerization of methacrylate derivatives, such as poly(γ-methacryloxypropyltrimethoxysilane) (PγMPS) [32] and poly{3-[tris-(trimethylsiloxy) silyl]propyl methacrylate} (PTRIS) [33].

At the beginning, we employed anhydrous ethanol as the solvent in the RAFT polymerization of DMA. To our disappointment, the conversion of DMA monomer remained extremely lower than expected, even lower than 25%. Consequently, isopropyl alcohol with relatively lower polarity was used to replace ethanol, and the higher monomer conversion was achieved successfully. The results of the DMA homopolymerization are listed in Table 1. Assuming each macromolecule contains one dithiobenzoate

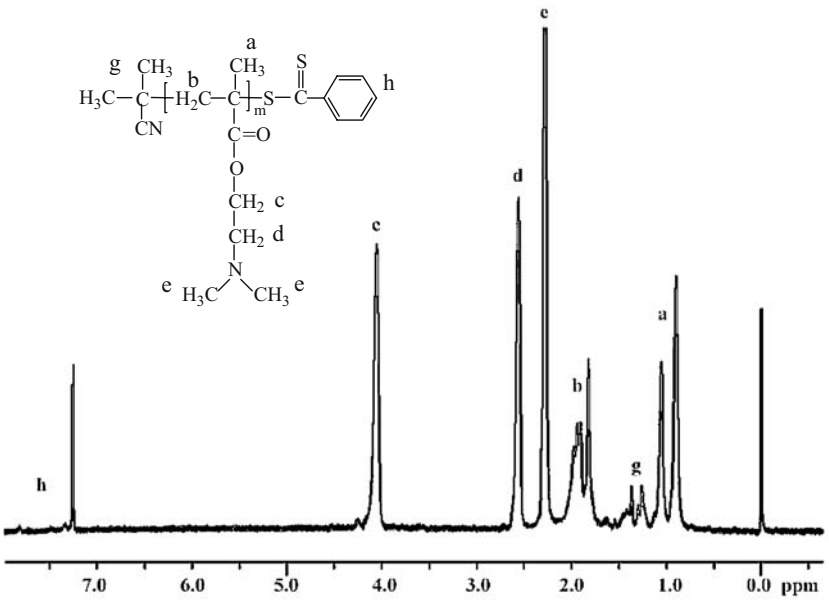

Fig. 1 ^1H NMR spectrum of PDMA homopolymer (M_n 2,950 g mol^{-1}, PDI 1.20) in $CDCl_3$

ester group, the theoretical number-average molecular weight ($M_{n,th}$) of the polymer could be calculated according to the following equation:

$$M_{n\_th} = [M]/[\mathrm{CTA}] \times M_{\mathrm{monomer}} \times \mathrm{conversion}(\%) + M_{\mathrm{CTA}}$$

where, for the homopolymers, [*M*] and [CTA] represent the initial concentration of DMA and CPDB, respectively. The monomer conversions are obtained by gravimetric method. M_{monomer} and M_{CTA} are the molecular weights of DMA and CPDB, respectively. While for the diblock copolymers, [*M*] and [CTA] are the initial concentration of SMA and PDMA macro-CTA, and conversion is the SMA conversion calculated from the ^{1}H NMR spectrum.

In general, for PDMA homopolymers, the experimental molecular weight (M_n) is below the theoretical one ($M_{n,th}$), as shown in Table 1. This phenomenon was also found by Claverie et al. [34] and not surprising, since in the calculation of $M_{n,th}$, the contribution of initiator-derived chains and thermally generated chains become significant. However, all the PDI values remained low, which indicated the well control behavior of the RAFT process.

In order to determine the chemical structure, composition, and molecular weights of the homopolymers, ^{1}H NMR measurement was carried out. Figure 1 shows the ^{1}H NMR spectrum of dithiobenzoate-capped PDMA homopolymer. The signal around δ 1.3 ppm corresponds to the protons of methyl group of the end 2-cyanoprop-2-yl group, and the peak at δ 7.2–7.9 ppm can be ascribed to the aromatic protons. The chemical shifts at δ 4.1 ppm, 2.6 ppm, and 2.3 ppm are attributed to the methylene protons adjacent to the oxygen atom (–OC$\boldsymbol{H}_2$–), the methylene protons adjacent to the nitrogen atom (–C$\boldsymbol{H}_2$N<), and the protons of the dimethylamino group –N(C$\boldsymbol{H}_3$)$_2$, respectively. These results indicate that CPDB reacted with primary or propagating radicals, and that the CPDB moiety remained at one end of the polymer chain.

For the RAFT polymerizations of DMA monomer with varying molar ratios of [*M*]/[CTA]/[I], Fig. 2a depicts the pseudo-first-order kinetic plots, and Fig. 2b shows the evolutions of molecular weights (M_n) and polydispersity (PDI) with conversions. From Fig. 2a, an inhibition time of about 40 min was observed. In fact, the inhibition period can hardly reach zero because the RAFT polymerization is subject to an initial period of slow polymerization. Barner–Kowollik et al. [35] attributed this phenomenon to two reasons: firstly, the slow fragmentation of the intermediate RAFT radicals in the preequilibrium; secondly, the slow reinitiation ability of the leaving group. After the inhibition time, the approximately linear first-order plots were gained, indicating that the polymerization is of living character. Figure 2b shows the plots demonstrating the evolution of number average molecular weight (M_n) versus the extent of

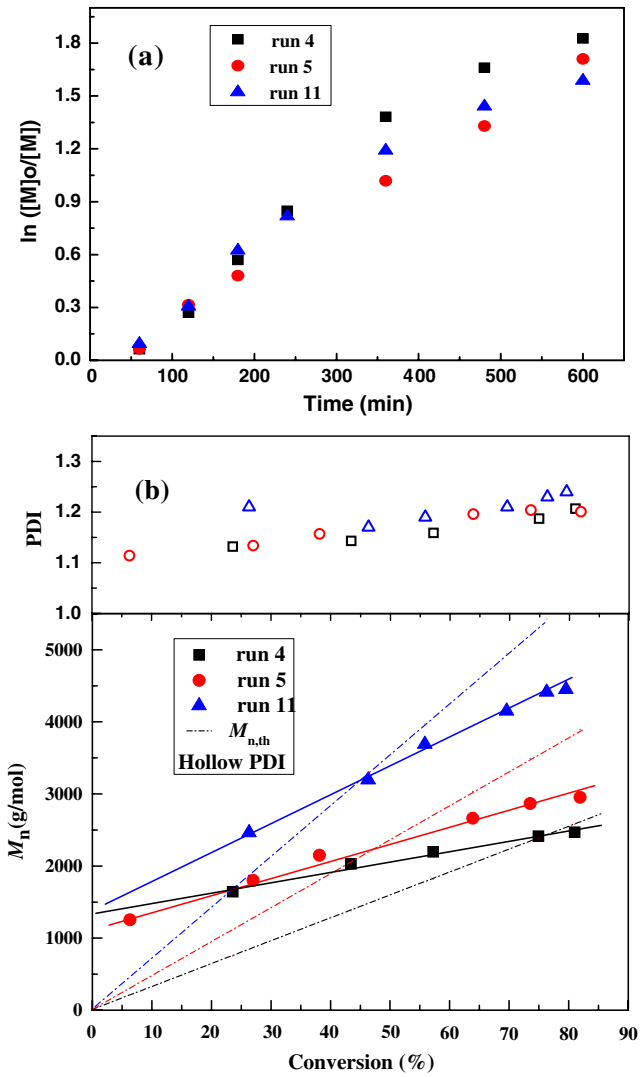

Fig. 2 RAFT polymerization of DMA with three different molar ratios of [*M*]/[CTA]/[I]: **a** first-order kinetic plots; **b** evolutions of molecular weights (M_n) and polydispersity (PDI) with conversions. Reaction conditions were as described in Table 1

polymerization along with the change in polydispersity (PDI). It is apparent that M_n values linearly increased up to quantitative monomer consumption, and PDI remained lower than 1.24 throughout the polymerization in all cases. However, the experimental trend lines are higher than the theoretical lines at lower monomer conversion and lower than the theoretical lines as the monomer conversion increased; moreover, the extrapolated lines cross the M_n axis between 1,000 and 1,400 Da at zero conversion. Similar observations have been previously reported in several literatures [12, 16, 36–38]. While the initial higher than expected M_n values may be due to some uncontrolled or normal free radical polymerization or caused by the calculated method of $M_{n,th}$ (the RAFT agent was slowly consumed, however, the $M_{n,th}$ was calculated based on the entire consumption of the RAFT agent), they attributed the

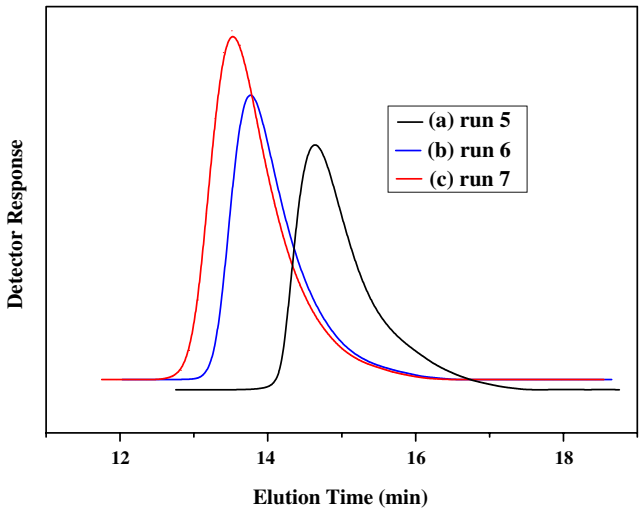

Fig. 3 GPC curves for the PDMA macro-CTA and PDMA-*b*-PSMA diblock copolymers obtained by chain extension reaction. **a** $PDMA_{17}$ (Run 5 in Table 1), M_n=2,950, PDI=1.20; **b** $PDMA_{17}$-*b*-$PSMA_{12}$ (Run 6 in Table 1), M_n=6,940, PDI=1.21; **c** $PDMA_{17}$-*b*-$PSMA_{17}$ (Run 7 in Table 1), M_n=8,640, PDI=1.26

observed discrepancy to calibration error in the GPC analysis. Likewise, in this study, we also think that the discrepancy between the measured M_n values and the theoretical ones was partly caused by polystyrene calibration standard.

Synthesis of diblock copolymers utilizing PDMA macro-CTA

To further investigate the RAFT mechanism of these polymerizations, chain extension reaction with the second monomer (SMA) was performed in the presence of the PDMA macro-CTA (M_n=2,950, PDI=1.20; M_n=3,110, PDI=1.20; M_n=4,450, PDI=1.24) to allow the formation of the PDMA-*b*-PSMA diblock copolymers. The experimental results are listed in Table 1.

Figure 3 describes the typical GPC plots of the PDMA macro-CTA homopolymer and PDMA-*b*-PSMA diblock copolymers. The curve b and c of the diblock copolymers ($PDMA_{17}$-*b*-$PSMA_{12}$ and $PDMA_{17}$-*b*-$PSMA_{17}$) move toward higher molecular weights compared with the first

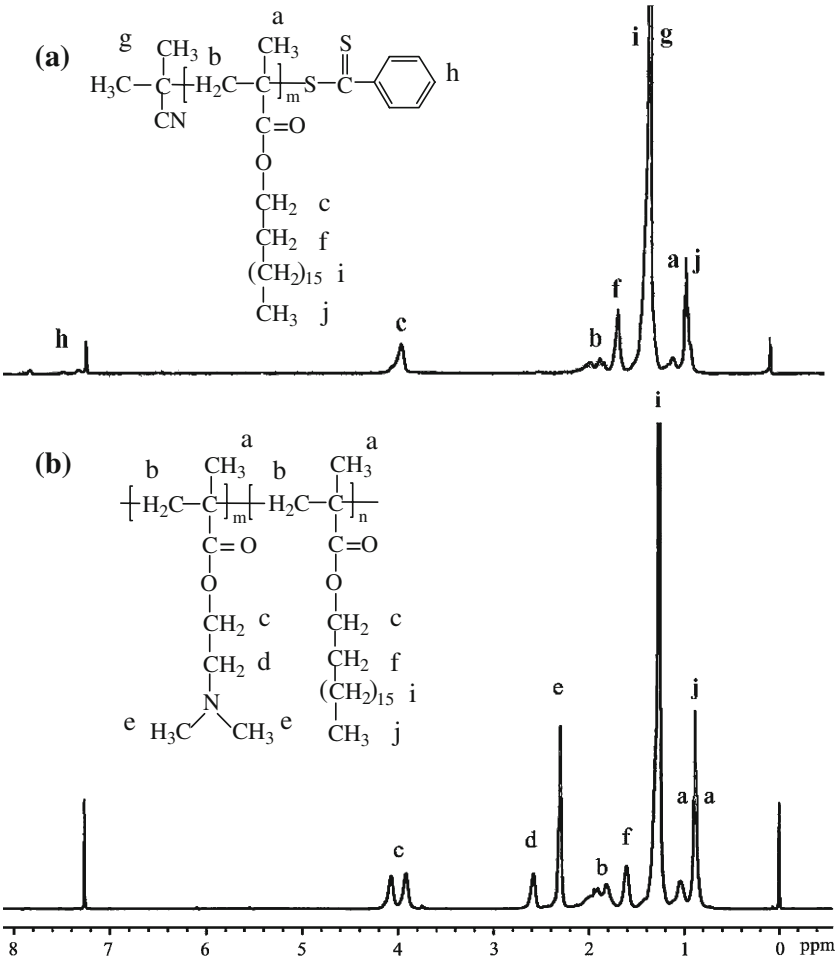

Fig. 4 ^{1}H NMR spectra of **a** PSMA homopolymer and **b** $PDMA_{17}$-*b*-$PSMA_{12}$ diblock copolymer (M_n=6,940 g mol^{-1}, PDI=1.21) in $CDCl_3$

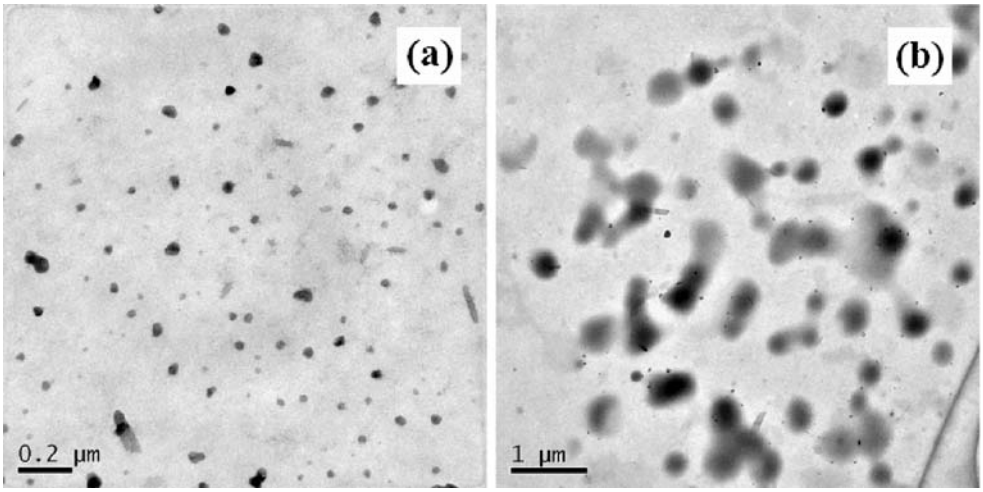

Fig. 5 TEM images of the aggregates made from $PDMA_{17}$-*b*-$PSMA_{12}$ (Run 6 in Table 1) at the polymer concentration of 0.1 wt.% in THF/water 90/10 (*w*/*w*) at various pH values: **a** pH 3.0, **b** pH 7.0

block PDMA macro-CTA homopolymer (curve a). The corresponding molecular weight distributions (PDIs) vary from 1.20 to 1.21 and 1.26. These results proved that chain extension occurred with near-quantitative blocking efficiency, indicating that almost all of the ends in the original PDMA macro-CTA chain remained active. Consequently, CPDB is an effective chain transfer agent for the polymerization of DMA and allows each terminal group of PDMA chain possesses dithiobenzoate group.

In order to confirm the chemical structure of PDMA-*b*-PSMA diblock copolymer, we used ^{1}H NMR spectroscopy to make a comparison with the PSMA homopolymer. Figure 4a,b exhibits the typical ^{1}H NMR spectra of PSMA homopolymer and PDMA-*b*-PSMA diblock copolymer, respectively. Comparing Fig. 1 with Fig. 4, we can find that all the signals of chemical shifts of the peaks corresponding to the protons in PDMA-*b*-PSMA copolymer can be found in Fig. 4b. The signals at δ 3.8–4.2 ppm can be attributed to the protons of methylene group (–C$\boldsymbol{H}_2$O–) adjacent to the oxygen atom in both PDMA and PSMA segments. The chemical shift of protons of methylene groups [–(C$\boldsymbol{H}_2$)$_{16}$–] in PSMA chain appears at δ 1.3 ppm, while the characteristic peak of the protons of the dimethylamino group –N(C$\boldsymbol{H}_3$)$_2$ in PDMA segment appears at δ 2.3 ppm. The illustrations made it apparent that the chain extension reaction of PSMA using PDMA as macro-CTA was achieved successfully.

Self-assembly behaviors of PDMA-*b*-PSMA in selective solvent

The morphology of self-assembly aggregates of copolymers is influenced mainly by several factors, such as the copolymer composition, the property of solvent, pH values,

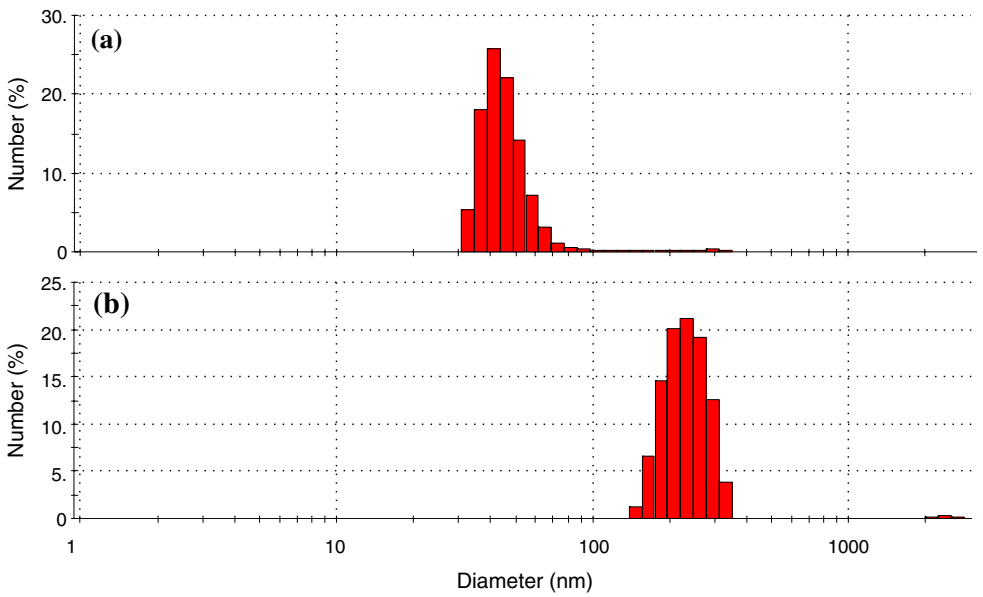

Fig. 6 Particle size analyses of the $PDMA_{17}$-*b*-$PSMA_{12}$ copolymer (Run 6 in Table 1) with the polymer concentration of 0.1 wt.% in THF/water 90/10 (*w*/*w*) at various pH values: **a** pH 3.0, **b** pH 7.0

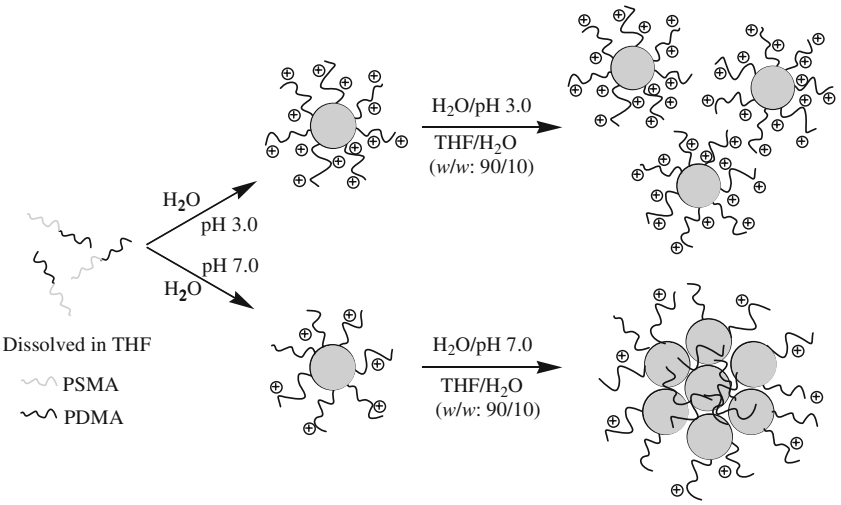

Fig. 7 Representative schematic models of different morphologies obtained by the self-assembly of $PDMA_{17}$-*b*-$PSMA_{12}$ (Run 6 in Table 1) with the polymer concentration of 0.1 wt.% in THF/water 90/10 (*w*/*w*) at various pH values: pH 3.0 and pH 7.0

and temperature [28, 30, 39, 40]. In the present paper, we have considered the effect of pH values, the copolymer composition and THF/water mixed solvent (weight ratios, *w*/*w*) on the morphologies of aggregates formed by PDMA-*b*-PSMA copolymers.

It should be noted that due to the high composition of the hydrophobic PSMA blocks, the relevant copolymer cannot be dispersed into water directly. However, the copolymer can be first dissolved in THF, which is a good solvent for both PDMA and PSMA blocks. Therefore, as

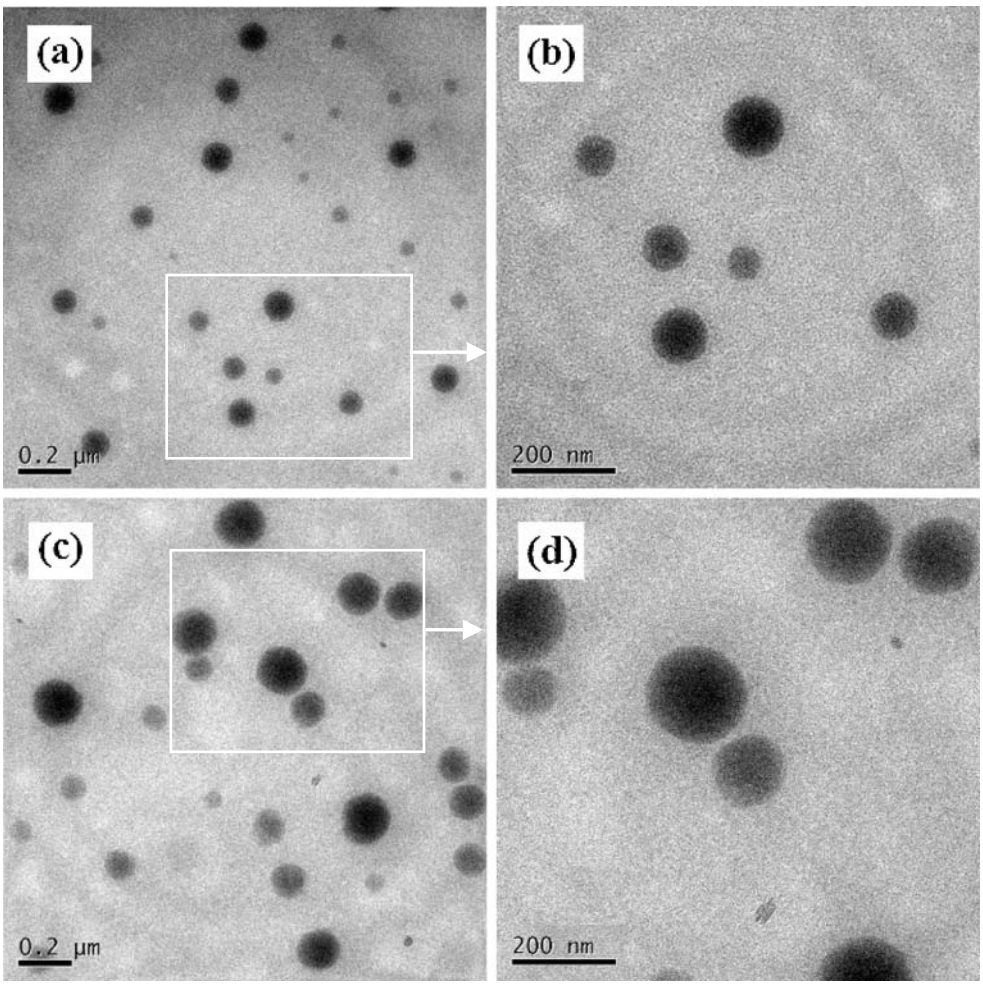

Fig. 8 TEM images of the aggregates formed from PDMA-*b*-PSMA with different copolymer compositions at polymer concentration of 0.3 wt.% in THF/water 90/10 (*w*/*w*), pH 7.0. **a, b** $PDMA_{18}$-*b*-$PSMA_{13}$ (Run 9 in Table 1) and **c, d** $PDMA_{18}$-*b*-$PSMA_{27}$ (Run 10 in Table 1)

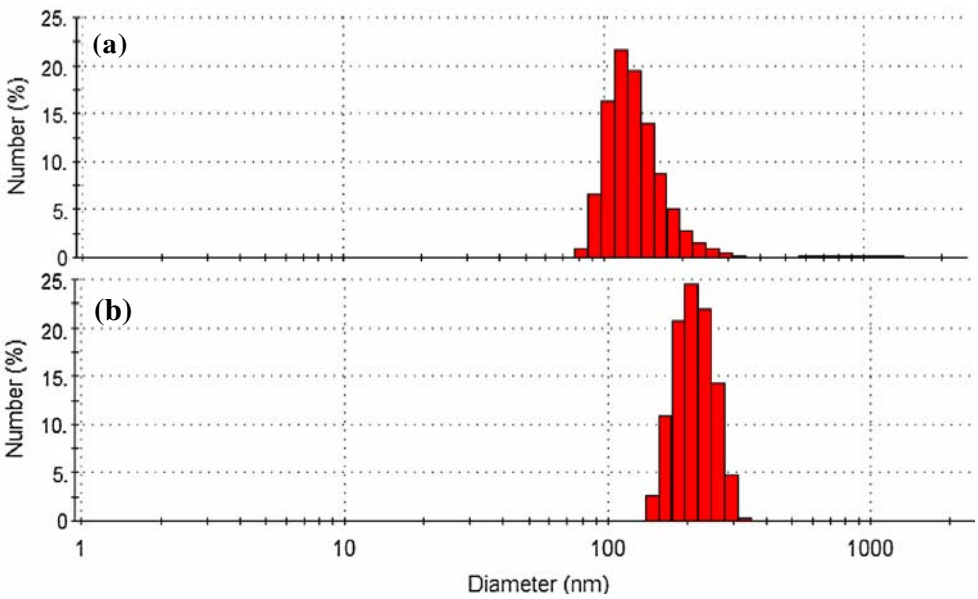

Fig. 9 Particle size analyses of PDMA-*b*-PSMA with different copolymer compositions at polymer concentration of 0.3 wt.% in THF/water 90/10 (*w*/*w*), pH 7.0. **a** $PDMA_{18}$-*b*-$PSMA_{13}$ (Run 9 in Table 1) and **b** $PDMA_{18}$-*b*-$PSMA_{27}$ (Run 10 in Table 1)

water is added slowly, the PSMA blocks are segregated from the increasingly aqueous environment, and aggregation occurs. During this progress, equilibrium exists between aggregated and free molecules [41].

Figure 5 shows the TEM images of aggregates from the $PDMA_{17}$-*b*-$PSMA_{12}$ copolymer solution with the copolymer concentration of 0.1 wt.% in THF/water (90/10, *w*/*w*) at different pH media. From Fig. 5a, one can observe that the diameter of micelles is about 20 nm at pH 3.0, whereas the aggregates go into larger ones with a diameter of around 200 nm at pH 7.0, as shown in Fig. 5b, because of the increasing aggregation numbers. Furthermore, to make sure the size of these aggregates in solution, particle size measurements were performed by dynamic light scattering (DLS), and the data of size distribution histograms are shown in Fig. 6. We can find that most of the aggregates are located in a relatively narrow range, and the average particle sizes of these aggregates are 40 nm at pH 3.0, and 233 nm at pH 7.0, respectively. Both average sizes were bigger than those observed by TEM (see Fig. 5), which was attributed to the stretch of the corona of aggregates in the solution, while TEM measurement showed the dried aggregates.

Considering the chemical structure of $PDMA_{17}$-*b*-$PSMA_{12}$, the dimension of these aggregates at pH 7.0 is very large. If the $PDMA_{17}$-*b*-$PSMA_{12}$ chains fully stretched out in the solution, the diameter of these aggregates should not exceed 15 nm=17×2×0.25 nm (the PDMA blocks) + 12×2×0.25 (the PSMA blocks) + 2×0.25 nm (the dithiobenzoate group). This theoretical diameter is quite close to that at pH 3.0 in Fig. 5a, but much smaller than the diameter of polymer aggregates at pH 7.0. Thus, the resultant aggregates at pH 3.0 should be simple micelles, while at pH 7.0 some PDMA blocks must be located inside the core of the aggregates to form a structure analogous to large compound micelles (LCMs). Eisenberg et al. have reported LCMs formed from

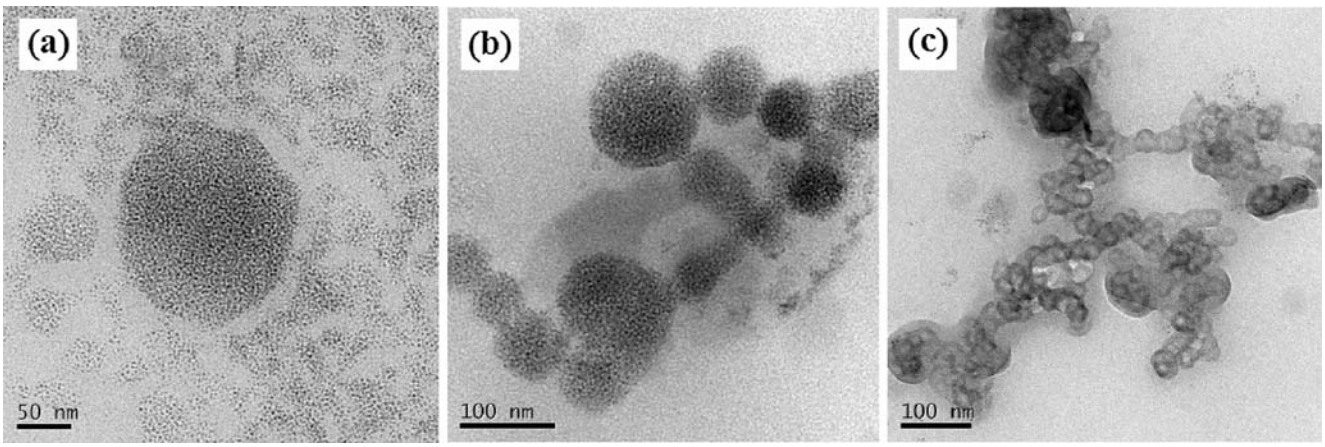

Fig. 10 TEM images of the aggregates formed by $PDMA_{17}$-*b*-$PSMA_{17}$ (Run 7 in Table 1) at the polymer concentration of 0.1 wt.% in THF/water mixed solvent. Deionized water content (wt.%): **a** 10, **b** 30, and **c** 50

linear copolymers of PS-*b*-PTMEACl (S: styrene; TMEACl: *N*, *N*, *N*-trimethylammoniumethylene acrylamide chloride) and explained them in detail [41]. According to the above studies, a possible aggregating mechanism for the self-assembly of the $PDMA_{17}$-*b*-$PSMA_{12}$ copolymer at different pH values is proposed as shown in Fig. 7. Under the condition of low pH value (pH 3.0), the PDMA block is completely protonated, and the electrostatic repulsion between protonized PDMA chains is strong. So the copolymer can only self-assemble into small micelles with the hydrophobic PSMA segments as the core and the protonated PDMA segments as the corona. However, as the pH value is increased to 7.0, the PDMA segments are partially deprotonated to become hydrophobic, so these deprotonated PDMA parts, and hydrophobic PSMA blocks could aggregate to create a continuous phase with islands of PDMA blocks nested throughout, leading to the formation of larger aggregates.

The composition of the copolymer is another effective approach to influence the morphology of aggregates. As shown in Fig. 8, for $PDMA_{18}$-*b*-$PSMA_{13}$ copolymers, the diameters of the aggregates are about 60~110 nm at the polymer concentration of 0.3 wt.% in THF/water 90:10 (*w*/*w*), whereas for $PDMA_{18}$-*b*-$PSMA_{27}$, the copolymers form larger aggregates with diameters about 100~190 nm under the same self-assembly condition. This change of the dimension of aggregates, as the length of hydrophobic block PSMA in PDMA-*b*-PSMA copolymer is increased from 13 to 27 units, is expectable. With the PSMA block length increasing, which means the increase of the core radius, the diameter of the aggregates must be enlarged. DLS was also used to investigate the aggregation behavior of PDMA-*b*-PSMA in THF/water. As shown in Fig. 9, the average particle sizes of these aggregates are 134 nm for $PDMA_{18}$-*b*-$PSMA_{13}$, and 215 nm for $PDMA_{18}$-*b*-$PSMA_{27}$, respectively. These results were in accordance with the TEM pictures (Fig. 8), considering the different conditions under which the TEM pictures and DLS histograms were obtained. Also, the aggregating mechanism for these copolymers is similar to the above schematic model at pH 7.0 in Fig. 7.

It's well-known that the water content in the polymer solution determines not only the onset of micellization, but also the shape and size of the formed aggregates. For example, as Eisenberg et al. reported, in a solution of 1.0% (*w*/*w*) PSt_{310}-*b*-PAA_{52} in dioxane, water addition induced a transition from spherical micelles, to mixtures of spheres and rods, to rods, to mixtures of rods and vesicles and finally to vesicles [39]. In our study, as shown in Fig. 10, $PDMA_{17}$-*b*-$PSMA_{17}$ aggregates also exhibited various morphologies in THF/water with different water contents. From Fig. 10a, we can observe that small micelles with average diameters of ca. 3 nm were formed at the water content of 10 wt.%. As the water content increased to 30 wt.%, it can be found that small micelles tend to concentrate together into large spheres as shown in Fig. 10b. With a further increase in water content to 50 wt.%, as shown in Fig. 10c, the morphology changes from large spheres into vesicles.

Eisenberg [39] et al. pointed out that the morphological transitions by adding water can be explained in terms of the effect of water on three factors: the core-chain stretching, corona-chain repulsion, and interfacial tension. When water was added into the initial solution to the critical water concentration (cwc), the copolymer molecules transformed from free chains to small micelles. After micellization, if the water content was increased, the interfacial tension would increase since the solvent became ill for the hydrophobic block. As a result, the system tended to increase the aggregate numbers to larger aggregates. However, the increase in the aggregates size was accompanied by the thermodynamically unfavorable increase in core-chain stretching and corona-chain repulsion. With further increases in the water content, in order to reduce the total free energy of the system, larger spherical aggregates underwent a morphological transition into vesicles.

Conclusions

In this article, a series of novel amphiphilic diblock copolymers of PDMA-*b*-PSMA with different molecular weights were prepared via RAFT/solution polymerization. The results obtained by ^{1}H NMR and GPC proved the success of the RAFT polymerization, and the PDIs of (co) polymers were fairly narrow. The self-aggregating structures of amphiphilic diblock copolymers with the concentration of 0.1~0.3 wt.% in THF/water mixed solvent was investigated by TEM and DLS measurements. It was found that the morphology of aggregates changed with the pH values, and the chain lengths of hydrophobic PSMA block also influenced on the size of aggregates. Furthermore, as the water content increased, the morphology of aggregates changed from small micelles to larger spheres, and then to vesicles.

Acknowledgements The authors gratefully acknowledge the financial support of the National Natural Science Foundation of China (No. 20474041) and the Natural Science Foundation of Jiangsu Province, China (BK2008157).

References

1. Krämer M, Stumbé J-F, Türk H, Krause S, Komp A, Delineau L, Prokhorova S, Kautz H, Haag R (2002) Angew Chem Int Ed 41:4252

2. Sheihet L, Dubin RA, Devore D, Kohn J (2005) Biomacromolecules 6:2726
3. Finne A, Andronova N, Albertsson A-C (2003) Biomacromolecules 4:1451
4. Lei L, Gohy J-F, Willet N, Zhang J-X, Varshney S, Jérôme R (2004) Macromolecules 37:1089
5. Du RH, Zhao JS (2004) J Membrane Sci 239:183
6. Mahltig B, Müller-Buschbaum P, Wolkenhauer M, Wunnicke O, Wiegand S, Gohy J-F, Jérôme R, Stamm M (2001) J Colloid Interf Sci 242:36
7. van de Wetering P, Cherng J-Y, Talsma H, Hennink WE (1997) J Control Release 49:59
8. Zhang YL, Xu L, Yi M, Zhai ML, Wang JR, Ha HF (2006) Eur Polym J 42:2959
9. Xin XQ, Wang YM, Liu W (2005) Eur Polym J 41:1539
10. Chong YK, Le TPT, Moad G, Rizzardo E, Thang SH (1999) Macromolecules 32:2071
11. Fijten MWM, Paulus RM, Schubert US (2005) J Polym Sci A Polym Chem 43:3831
12. Sahnoun M, Charreyre M-T, Veron L, Delair T, D'Agosto F (2005) J Polym Sci A Polym Chem 43:3551
13. Xiong QF, Ni PH, Zhang F, Yu ZQ (2004) Polym Bull 53:1
14. Cheng W, Fan X, Liu Y, Tian W (2006) Polym Mater Sci Eng 22:88
15. Fournier D, Hoogenboom R, Thijs HML, Paulus RM, Schubert US (2007) Macromolecules 40:915
16. Lowe AB, Wang R (2007) Polymer 48:2221
17. Li Y, Smith AE, Lokitz BS, McCormick CL (2007) Macromolecules 40:8524
18. Liu QQ, Yu ZQ, Ni PH (2004) Colloid Polym Sci 282:387
19. Ni PH, Zhang MZ, Ma LH, Fu SK (2006) Langmuir 22:6016
20. Xu J, Ni PH, Mao J (2006) e-Polymers No.015:1
21. Mao J, Ni PH, Mai YY, Yan DY (2007) Langmuir 23:5127
22. Zhang H, Ni PH, He JL, Liu CC (2008) Langmuir 24:4647
23. Baskar G, Ramya S, Mandal AB (2002) Colloid Polym Sci 280:886
24. Qin SH, Saget J, Pyun J, Jia SH, Kowalewski T, Matyjaszewski K (2003) Macromolecules 36:8969
25. Pitsikalis M, Siakali-Kioulafa E, Hadjichristidis N (2000) Macromolecules 33:5460
26. Zhou JF, Wang L, Dong XC, Yang Q, Wang JJ, Yu HJ, Chen X (2007) Eur Polym J 43:1736
27. Zhou JF, Wang L, Yang Q, Dong X, Yu H (2007) Colloid Polym Sci 285:1369
28. Zhou JF, Wang L, Yang Q, Liu Q, Yu H, Zhao Z (2007) J Phys Chem B 111:5573
29. Schilli CM, Zhang MF, Rizzardo E, Thang SH, Chong YK, Edwards K, Karlsson G, Muller AHE (2004) Macromolecules 37:7861
30. Cohen Stuart MA (2008) Colloid Polym Sci 286:855
31. Moad G, Chiefari J, Chong YK, Krstina J, Mayadunne RTA, Postma A, Rizzardo E, Thang SH (2000) Polym Int 49:993
32. Mellon V, Rinaldi D, Bourgeat-Lami E, D'Agosto F (2005) Macromolecules 38:1591
33. Saricilar S, Knott R, Barner-Kowollik C, Davis TP, Heuts JPA (2003) Polymer 44:5169
34. Uzulina I, Gaillard N, Guyot A, Claverie J (2003) C R Chimie 6:1375
35. Vana P, Davis TP, Barner-Kowollik C (2002) Macromol Theory Simul 11:823
36. Albertin L, Stenzel M, Barner-Kowollik C, Foster LJR, Davis TP (2004) Macromolecules 37:7530
37. Ohno K, Tsujii Y, Miyamoto T, Fukuda T (1998) Macromolecules 31:1064
38. Chen YM, Wulff G (2001) Macromol Chem Phys 202:3426
39. Choucair A, Eisenberg A (2003) Eur Phys J E 10:37
40. Peng D, Zhang XH, Huang XY (2006) Polymer 47:6072
41. Cameron NS, Eisenberg A, Brown GR (2002) Biomacromolecules 3:124